THE JOURNAL OF BIOLOGICAL CHEMISTRY
Vol. 279, No. 18, Issue of April 30, pp. 18944–18951, 2004
Printed in U.S.A.

Bacterial Penetration of Bladder Epithelium through Lipid Rafts*

Received for publication, January 23, 2004, and in revised form, February 18, 2004
Published, JBC Papers in Press, February 19, 2004, DOI 10.1074/jbc.M400769200

Matthew J. Duncan‡, Guojie Li§, Jeoung-Sook Shin§, Johnny L. Carson¶, and Soman N. Abraham‡§‖**

From the ‡Department of Molecular Genetics and Microbiology and the §Department of Pathology, Duke University Medical Center, Durham, North Carolina 27710, the ¶Department of Cell and Developmental Biology, University of North Carolina, Chapel Hill, North Carolina 27599, and the ‖Department of Immunology, Duke University Medical Center, Durham, North Carolina 27710

Type 1 fimbriated *Escherichia coli* represents the most common human uropathogen, owing much of its virulence to invasion of the uroepithelium, which is highly impermeable due to the preponderance of uroplakins and highly ordered lipid components. We sought to elucidate the molecular basis for *E. coli* invasion of the bladder epithelium by employing human 5637 bladder epithelial cells, and we found the following: (i) intracellular *E. coli* associated with caveolae and lipid raft components; (ii) RNA_i reduction of caveolin-1 expression inhibited bacterial invasion; (iii) a signaling molecule required for *E. coli* invasion was located in lipid rafts and physically associated with caveolin-1; (iv) bacterial invasion was inhibited by lipid raft disrupting/usurping agents. In the mouse bladder, the *E. coli* type 1 fimbrial receptor, uroplakin Ia, was located in lipid rafts, and lipid raft disruptors inhibited *E. coli* invasion. Cumulatively, *E. coli* uroepithelial invasion occurs through lipid rafts, which, paradoxically, contribute to bladder impermeability.

Urinary tract infections (UTIs),[1] one of the most common bacterial infections in humans, cause 6–7 million hospital visits per year (1, 2). The most common causative agent of UTIs is uropathogenic *Escherichia coli* (2, 3), which expresses filamentous organelles of adhesion called type 1 fimbriae (4). These fimbriae mediate bacterial adherence to the uroepithelium, promoting sustained colonization of this normally sterile body site (5). An important characteristic of UTIs is the frequency of recurrence among women (6), as up to 25% of women who experience a first UTI will have a second infection within 6 months (7). Historically, recurrence was thought to be initiated by a reinfection of the urinary tract from a reservoir of uropathogenic bacteria located in the gastrointestinal tract (8). However, recently it has been shown that *E. coli* can survive for many weeks in the bladders of mice, without bacteriuria (9, 10). This establishment of a quiescent bladder infection has been linked to the ability of type 1 fimbriated *E. coli* to invade and persist within bladder epithelial cells (BEC). Invasion was mediated by bacterial type 1 fimbriae (11), and in their intracellular location, the bacteria were presumably inaccessible to immune cells of the host as well as antibiotics (9, 10). The ability of *E. coli* to invade and persist within BEC could explain the frequent recurrence of *E. coli* infections of the bladder and their apparent resistance to antibiotic therapy.

It is interesting that the typically noninvasive uropathogenic *E. coli* is able to invade the bladder epithelium, considering the highly impermeable barrier it presents to its luminal contents (12, 13). It has been shown recently that the high impermeability of the urothelium arises largely from the presence of scallop-shaped plaques on the apical surface of the superficial BEC, also known as the asymmetric unit membrane, which line the lumen of the bladder (13, 14). These plaques are composed of four subunits, known as uroplakins (UP): UPIa, the host receptor for type 1 fimbriated *E. coli* (15), and UPIb, which pair with UPII and UPIII, respectively (16). The composition of the lipids associated with the urothelial plaques is also believed to play a large role in determining the permeability barrier of the uroepithelium (14, 17). Purified urothelial plaques are rich in both cholesterol and sphingolipids (18, 19), which leads to a more ordered lipid structure, lowering membrane fluidity and permeability and favoring microdomain formation (20–22). Thus, the urothelial plaques work in conjunction with associated specialized lipid microdomains to mediate the high impermeability of the uroepithelium. Cholesterol- and sphingolipid-enriched microdomains have recently been the focus of much study and are often referred to as lipid rafts (20, 22, 23).

Lipid rafts are highly ordered regions of the plasma membranes enriched in not only cholesterol and sphingolipids but also glycolipids and glycosylphosphatidylinositol-anchored molecules and may contain a 22-kDa protein, caveolin-1 (20, 23, 24). A subtype of lipid rafts, caveolae, has a distinct cave-like morphology in the plasma membrane (23, 25). Lipid rafts have been implicated in signal transduction as a large number of signaling molecules aggregate within them (20, 23, 24). These microdomains also possess a versatile endocytic capacity that has been implicated recently in microbial pathogenesis as demonstrated by their ability to mediate the entry of viruses, bacteria, and even large parasites into host cells (25, 26). Paradoxically, *E. coli* may be using the very same structures that mediate the highly impermeable nature of the uroepithelium, namely urothelial plaques (specifically UPIa) and the cholesterol/sphingolipid-rich membrane microdomains associated with them, to penetrate the uroepithelial barrier. We tested this hypothesis by investigating the role of lipid rafts in type 1

* This work was supported by National Institutes of Health Grants R37-DK50814 and RO1-AI50021 and a Senior Investigator award from the Sandler Family Foundation on Asthma Research. The costs of publication of this article were defrayed in part by the payment of page charges. This article must therefore be hereby marked "*advertisement*" in accordance with 18 U.S.C. Section 1734 solely to indicate this fact.

** To whom correspondence should be addressed: Dept. of Pathology, Duke University Medical Center, Box 3712, Durham, NC 27710. Tel.: 919-684-3630; Fax: 919-684-2021; E-mail: soman.abraham@duke.edu.

[1] The abbreviations used are: UTI, urinary tract infection; BEC, bladder epithelial cells; CTB, cholera toxin B subunit; MBCD, methyl-β-cyclodextrin; UP, uroplakin; TEM, transmission electron microscopy; RNA_i, RNA interference; MTT, 3-(4,5-dimethylthiazol-2-yl)-2,5-diphenyltetrazolium bromide; PMSF, phenylmethylsulfonyl fluoride; PBS, phosphate-buffered saline; MES, 4-morpholineethanesulfonic acid; FITC, fluorescein isothiocyanate; RT, room temperature; EGFP, enhanced green fluorescent protein.

fimbriated *E. coli* invasion of BEC, as elucidation of the molecular aspects of *E. coli* entry into BEC could lead to the development of effective strategies to prevent the emergence and recurrence of UTIs.

EXPERIMENTAL PROCEDURES

Bacteria and Cell Lines—*E. coli* strain ORN103 (27), containing a complete deletion of the type 1 fimbrial gene cluster, was transformed with plasmid pSH2 (type 1 fimbrial gene cluster, chloramphenicol resistance) (27) or plasmid pREP4 (kanamycin resistance) (Qiagen, Valencia, CA). Bacteria were grown in 10 ml of static Luria-Bertani (LB) broth with the appropriate antibiotics for 24 h prior to use. Uropathogenic *E. coli* J96 (28) was grown in 10 ml of static Luria-Bertani (LB) broth for 24 h in the absence of antibiotics. Type 1 fimbrial expression was confirmed by mannose-sensitive agglutination of baker's yeast. *Listeria monocytogenes* was grown overnight in brain heart infusion broth (BD Biosciences). The human bladder epithelial cell line 5637 (ATCC HTB-9) was grown in RPMI 1640 (Invitrogen) supplemented with 10% fetal bovine serum (HyClone, Logan, UT), 2.0 g/liter sodium bicarbonate, 0.3 g/liter L-glutamine, 2.5 g/liter glucose, 10 mM HEPES, and 1 mM sodium pyruvate. Cells were cultured at 37 °C with 5% CO_2.

5637 BEC Uroplakin Ia Expression—5637 BEC lysates (~8.0×10^6 cells) were made in 400 μl of 2× Laemmli sample buffer (Bio-Rad) and either boiled for 5 min or allowed to remain at room temperature (RT) for 30 min before SDS-PAGE (45 μl of each sample), transfer to a polyvinylidene difluoride membrane, and immunoblotting with a UPIa-specific polyclonal antibody (Santa Cruz Biotechnology, Santa Cruz, CA).

In Vitro Bacterial Invasion Assays—5637 bladder epithelial cells were seeded into 96-well plates and grown to confluence. Bladder cells were infected at a multiplicity of infection of 50–100 bacteria per host cell by the addition of 100 μl of bacteria diluted in serum-free cell culture medium containing 10 mg/ml bovine serum albumin (Sigma), A_{600} ~0.05. Plates were centrifuged for 5 min at 600 × *g* to accelerate bacterial contact with host cells. Plates were then incubated at 37 °C for 2 h, and the medium was replaced with fresh culture medium containing 100 μg/ml of the membrane-impermeable antibiotic gentamicin (Invitrogen) to kill extracellular bacteria. Incubation was continued for an additional 1 h, after which each well was washed three times with PBS and the cells were lysed by the addition of 100 μl of 0.1% Triton X-100 in PBS and plated onto LB agar plates with chloramphenicol for *E. coli* ORN103(pSH2) or brain heart infusion agar plates for *L. monocytogenes*.

To test the effect of specific caveolar disruptors/usurpers on bacterial invasion, methyl-β-cyclodextrin (1, 5, or 10 mM, Sigma) along with lovastatin (10 μM) in serum-free medium was added to the cells for 30 min prior to infection. The cells were washed three times to remove the methyl-β-cyclodextrin, and the medium was replaced with bacteria-containing medium along with 10 μM lovastatin. Nystatin (5 mg/ml stock in Me_2SO, Sigma) was added to the cells at a concentration of 50 μg/ml in serum-free medium for 30 min prior to infection. Nystatin was removed by washing three times, and the cells were infected as before. The B subunit of cholera toxin (CTB, Sigma) was preincubated with the cells for 30 min before infection at a concentration of 20 μg/ml and remained on the cells throughout the invasion assay. The viability of the bladder cells was not affected by any of the treatments used as determined by trypan blue exclusion. The MTT adherence assay was performed as follows. 5637 cells were plated overnight onto 96-well plates and then incubated with 0, 1, 5, or 10 mM methyl-β-cyclodextrin for 30 min as above and then fixed overnight with 2.5% paraformaldehyde. The monolayers were washed three times with sterile PBS and pretreated for 1 h at RT with blocking buffer (3% bovine serum albumin in PBS). 100 μl of ORN103(pSH2) (A_{600} ~1.0) in PBS was incubated with the monolayers for 1 h at RT. Nonadherent bacteria were removed by washing the cell monolayers three times with PBS. Fifty μl of LB was applied to each monolayer and incubated for 15 min at 37 °C. MTT (Sigma) was dissolved in PBS at 2 mg/ml, filter-sterilized, and stored at 4 °C until use. Fifty μl of 2 mg/ml MTT was added to all wells, and the plates were incubated for 15 min at 37 °C to allow reduction of MTT to formazan by live bacteria. 150 μl of isopropyl alcohol and hydrochloric acid (at a ratio of 24:1) was added to each well to solubilize the formazan and the absorbance was measured at 450 nm using a Tecan Sunrise remote microplate reader.

Bacterial Invasion of Mouse Bladder Epithelium in Vivo—For quantitative determination of bacterial invasion, 8-week-old female BALB/c mice were anesthetized with pentobarbital sodium and inoculated transurethrally with 50 μl of an *E. coli* J96 bacterial suspension (~1.0×10^8 colony-forming units) or a *L. monocytogenes* bacterial suspension (~1.0×10^7 colony-forming units) suspended in PBS with or without 25 mM methyl-β-cyclodextrin. After 1 h, bladders were aseptically removed, bisected, and incubated for 1 h in culture media with 100 μg/ml gentamicin followed by homogenization in 1 ml of sterile 0.1% Triton X-100. Serial dilutions of the homogenates were plated onto MacConkey agar plates (for *E. coli* J96) or brain heart infusion agar plates (for *L. monocytogenes*). Methyl-β-cyclodextrin had no effect on bacterial viability as determined by colony counts with or without a 60-min incubation in 25 mM methyl-β-cyclodextrin.

Sucrose Density Fractionation of Infected Bladder Epithelial Cells—Bladder epithelial cells were grown to confluence on OmniTray tissue culture plates (growth area ~110 cm^2, Nalge Nunc International, Rochester, NY). Three plates were infected with FITC-labeled *E. coli* ORN103(pSH2) in 15 ml of serum-free medium (1×10^9–2×10^9 bacteria per plate) for 2 h. Infected plates, along with three uninfected plates, were washed five times with ice-cold PBS and scraped off the plates using a rubber policeman in 1 ml of homogenization buffer (10 mM Tris (pH 7.2), 2 mM EDTA, 1 mM PMSF, and a 1:100 dilution of mammalian protease inhibitor mixture (Sigma)). The cell suspension was then passed 20 times through a 27-gauge needle, brought to 45% sucrose by the addition of an equal volume of 90% sucrose, and then overlaid with 2 ml each of 35, 25, 15, and 5% sucrose. The gradients were centrifuged for 18 h at 39,000 rpm in a SW41Ti rotor (Beckman Instruments, Palo Alto, CA), and 10 equal fractions were collected from the top of each gradient and assayed for caveolin-1 by Western blotting using polyclonal anti-caveolin-1 antibody (Transduction Laboratories, San Diego) and a goat anti-rabbit IgG conjugated to horseradish peroxidase (Sigma). The fractions were also assayed for fluorescence using a fluorometer.

Fluorescent Microscopy—5637 bladder epithelial cells were seeded onto 12-mm diameter glass coverslips placed into the wells of a 24-well plate and grown overnight. The cells were infected with ORN103(pSH2) as in the invasion assays. The infected cells were incubated at 37 °C for 1–2 h, washed four times with PBS to remove unbound bacteria (followed by an additional 1-h incubation with 20 μg/ml FITC-CTB (Sigma) for the cells to be examined for GM1 labeling), and fixed overnight in 2.5% paraformaldehyde in PBS. To label cholesterol, the cells were incubated with 200 μg/ml of the UV fluorescent cholesterol-binding fungal toxin filipin (Sigma) in PBS for 30 min. To examine caveolin-1 labeling, 5637 cells grown on coverslips as above were infected with the uropathogenic *E. coli* J96 for 1–2 h as in the invasion assays, washed three times with PBS, and fixed overnight with 2.5% paraformaldehyde. After removing the fixative, the cells were permeabilized with 0.1% Triton X-100 (Sigma), and caveolin-1 was then labeled using polyclonal anti-caveolin-1 antibody followed with goat anti-rabbit Alexa Fluor 488 $F(ab')_2$ (Molecular Probes). Coverslips were examined using a Nikon Eclipse TE200 microscope with a 4,6-diamidino-2-phenylindole filter set to examine filipin labeling and a fluorescein filter set to examine GM1 and caveolin-1 labeling.

Lipid Raft Purification—5637 BEC lipid rafts were purified using a method described previously with some modifications (29). Briefly, 5637 BEC grown to confluency on OmniTray tissue culture plates (growth area ~110 cm^2, Nalge Nunc International) were left untreated or treated with 10 mM methyl-β-cyclodextrin in serum-free RPMI 1640 (Invitrogen) at 37 °C for 1 h. Treated and untreated cells (two tissue culture plates per condition) were washed three times with ice-cold PBS and removed from the plates using rubber policeman in 3 ml of ice-cold PBS per plate. Treated and untreated cells were then collected by centrifugation, and each cell pellet was resuspended in 2 ml of ice-cold carbonate buffer (500 mM Na_2CO_3 (pH 11.00), 1 mM EDTA, 1 mM PMSF, and a 1:100 dilution of mammalian protease inhibitor mixture (Sigma)). The cells were homogenized by passing through a 21-guage needle 20 times, sonicated in an ice bath for 5 min, and passaged through a 21-guage needle an additional 20 times. The samples were brought to 45% sucrose by the addition of an equal volume of 90% sucrose in MBS (25 mM MES (Sigma), 75 mM NaCl, pH 6.8) and then overlaid with 4 ml each of 35 and 5% sucrose in MBS. The gradients were centrifuged for 18 h at 39,000 rpm in a SW41Ti rotor (Beckman Instruments, Palo Alto, CA), and 12 equal fractions (1 ml each) were collected from the top of each gradient and assayed for Rac1 and caveolin-1 by Western blotting using monoclonal anti-Rac1 (Transduction Laboratories) or polyclonal anti-caveolin-1 antibody.

Lipid rafts were purified from BALB/c mouse bladders as follows. Bladders from 15 BALB/c female mice were removed and washed briefly in ice-cold PBS, before brief homogenization in a Potter-Elvehjem tissue grinder (Kontes Glass Co., Vineland, NJ) in ice-cold PBS. The resulting suspension was filtered through a 70-μm cell strainer (BD Biosciences)

and collected by centrifugation. The pellet was resuspended in 1 ml of carbonate buffer and homogenized by passing through a 21-gauge needle 20 times, sonicated in an ice bath for 5 min, and passaged through a 21-gauge needle an additional 20 times. The sample was brought to 45% sucrose by the addition of an equal volume of 90% sucrose in MBS and then overlaid with 2 ml each of 35 and 5% sucrose in MBS. The gradient was centrifuged for 18 h at 39,000 rpm in a SW41Ti rotor, and 12 equal fractions (500 μl each) were collected from the top of each gradient and assayed for UPIa, caveolin-1, and clathrin heavy chain by Western blotting using polyclonal anti-UPIa, polyclonal anti-caveolin-1, or monoclonal anti-clathrin heavy chain (Transduction Laboratories) antibodies.

Immunoprecipitation—Caveolin-1 and Rac1 were immunoprecipitated from fraction 5 of the 5637 BEC lipid raft preparation as follows. 400 μl of fraction 5 was brought to 1 ml with MBS (1% Nonidet P-40, 1 mM PMSF, and a 1:100 dilution of mammalian protease inhibitor mixture). The sample was precleared with 10 μg of normal rabbit IgG (Santa Cruz Biotechnology) and 50 μl of a 50% suspension of protein G-Sepharose (Sigma) in MBS for 1 h at 4 °C. 4 μg of polyclonal anti-Rac1 (Santa Cruz Biotechnology) or polyclonal anti-caveolin-1 was added, and the sample was incubated for 16 h at 4 °C. 50 μl of a 50% suspension of protein G-Sepharose was added, and the sample was further incubated for 1 h at 4 °C. The immunoprecipitates were washed three times with 1 ml of MBS (1% Nonidet P-40, 1 mM PMSF, and a 1:100 dilution of mammalian protease inhibitor mixture), resuspended in 60 μl of 2× Laemmli sample buffer, and boiled for 5 min. Immunoprecipitates were assayed for Rac1 and caveolin-1 using monoclonal anti-Rac1 or polyclonal anti-caveolin-1 antibodies.

Construction of Small Interfering RNA Vector, Transfection, and Infection—To construct the small interfering RNA expression vector, the pEGFP-N1 (BD Biosciences) backbone was used. Briefly, pEGFP-N1 was digested by BglII and BamHI and was then re-ligated to generate pEGFP-N1A. Human U6 small nuclear RNA promoter was PCR-amplified from pTZ U6 + 1 (gift from John Rossi, Beckman Research Institute of the City of Hope, Duarte, CA) with added HindIII and BamHI sites at 5′ and 3′ ends, respectively. The PCR product was cloned into pUC18 to generate pUC18-U6. The U6 promoter and its flanking multiple cloning sites were PCR-amplified from pUC18-U6 with an added AflII site at both 5′ and 3′ ends. The PCR product was cloned into pEGFP-N1A by using its unique AflII site to generate pEGFP-N1A-U6. Oligo1, 5′-GATCCC**GGAGATCGACCTGGTCAAC**-TTCAAGAGAGTTGACCAGGTCGATCTCCTTTTTGGAAG-3′, and oligo2, 5′-AATTCTTCCAAAAAA**GGAGATCGACCTGGTCAAC**TCTCT-TGAAGTTGACCAGGTCGATCTCCGG-3′ were ordered from Integrated DNA Technologies, Inc. Coralville, IA. The boldface and underlined sequences are forward and reverse sequences, respectively, which correspond to nucleotides 419–437 of the human cavolin-1 gene (GenBank™ accession number NM-001753). Oligo1 and 2 were annealed to form double-stranded DNA and cloned into pEGFP-N1A-U6 by using BamHI and EcoRI sites to generate pSi-Cav419. pEGFP-N1A-U6 and pSi-Cav419 were used to transfect human bladder cell line 5637 by using LipofectAMINE 2000 (Invitrogen). Five days following transfection, the cells were plated onto 96-well plates and grown overnight, followed by the invasion assay using *E. coli* ORN103(pSH2) as described above. The transfected cells were also seeded onto glass coverslips and grown overnight, followed by paraformaldehyde fixation and labeling for caveolin-1 with polyclonal anti-caveolin-1 and goat anti-rabbit Alexa Fluor 660 $F(ab')_2$ (Molecular Probes). Endogenous caveolin-1 expression was examined using a Nikon Eclipse TE200 confocal scanning light microscope. Whole cell lysates of 5-day post-transfection cells were examined by Western blotting using polyclonal anti-caveolin-1 antibody as above or monoclonal anti-β-actin, clone AC-15 (Sigma), to control for protein loading. Densitometry was performed using ImageJ software (National Institutes of Health, rsb.info.nih.gov/ij/).

Electron Microscopy—Bladder epithelial cells grown on Transwell filters were left uninfected or infected with *E. coli* ORN103(pSH2) for 4 h, washed to remove unbound bacteria, and fixed with 2% paraformaldehyde, 2% glutaraldehyde in PBS. The filters were processed for TEM using standard methods. For the enumeration of caveolae, uninfected cells grown on Transwell filters and processed for TEM as above were examined, and caveolae were enumerated as described previously (30).

RESULTS

The 5637 Human BEC Line Expresses UPIa Protein—To begin studying the aspects of *E. coli* BEC invasion, we utilized a well established *in vitro* model, the 5637 human BEC line, that has been shown to closely mimic *E. coli*/BEC interactions *in vivo* (9, 11, 31–33). Although 5637 BEC have been used previously, they were never shown to express the protein UPIa, the *in vivo* host receptor for type 1 fimbriated *E. coli* (15). We therefore examined 5637 BEC for the expression of UPIa. Western blotting was performed on a whole cell lysate boiled in 2× Laemmli sample buffer, using a UPIa specific antibody. No band of the expected size (27 kDa) was seen, but a much larger, unclear band was observed, indicating that the protein may have been aggregated by boiling in Laemmli sample buffer, as reported previously for bovine UPI (Fig. 1*A*) (34). Another whole cell lysate was prepared and allowed to remain at room temperature for 30 min before SDS-PAGE and immunoblotting, and a single band of the appropriate size was seen, demonstrating that 5637 BEC express UPIa, the *in vivo* host cell receptor for *E. coli* type 1 fimbriae (Fig. 1*B*).

Morphological Aspects of E. coli Invasion—Transmission electron microscopy (TEM) was performed on uninfected and infected 5637 BEC monolayers, grown on Transwell filters, to explore the morphological aspects of *E. coli* invasion. Uninfected BEC were observed to express distinct cave-like structures, called caveolae, along their basolateral surface (218 basolateral caveolae/mm of filter), but none were visible on their apical surface, consistent with previous reports of polarized caveolae expression on other epithelial cell lines (Fig. 1*C*) (30). On BEC infected with type 1 fimbriated *E. coli*, caveolae were now found at the apical surface, intimately associated with invading bacteria at their point of attachment and forming part of the phagosomal structure encasing internalized bacteria (Fig. 1, *D–F*). As a means of further demonstrating lipid raft association with intracellular *E. coli*, we examined infected BEC using specific probes for the most commonly used markers of lipid rafts: caveolin-1, cholesterol, and the glycolipid GM1 (23, 35, 36). Shown in Fig. 2, *B*, *D*, and *F*, are fluorescent images showing the accumulation of caveolin-1, cholesterol, and GM1, respectively, around intracellular *E. coli*. The corresponding differential interference contrast images are shown in Fig. 2, *A*, *C*, and *E*. We also employed a biochemical approach to demonstrate mobilization of cellular caveolin-1 to sites of intracellular bacteria. FITC-labeled *E. coli* ORN103(pSH2) were incubated with BEC, after which the cells were homogenized and fractionated on a sucrose gradient to isolate intracellular bacteria-containing compartments as described previously (35). Each of the various fractions was collected and probed for fluorescence. Most of the fluorescence was associated with fractions 8–10, which represented extracellular bacteria (Fig. 2*G*). However, a small peak of fluorescence, representing bacteria-containing phagosomes, was detected in fraction 5. When fractions obtained from infected and uninfected BEC were probed with caveolin-1-specific antibody on a Western blot, the distribution of caveolin-1 was virtually identical except in fraction 5 of the infected cells, where a noticeable shift in cellular caveolin-1 to the location of intracellular bacteria was observed (Fig. 2*G*). Taken together, the microscopic and biochemical data point to the mobilization and colocalization of common lipid raft markers at sites of intracellular *E. coli*.

Caveolin-1 Is Essential for Optimal E. coli Invasion of BEC—If *E. coli* is utilizing lipid rafts for the invasion of BEC, it stands to reason that certain lipid raft-associated proteins would be required for entry through this pathway. Previously, the lipid raft-associated protein caveolin has been shown to be involved in the infection of host cells by various pathogens that enter cells via lipid rafts (37, 38). To examine the role of caveolin-1 protein in *E. coli* invasion of BEC, we utilized the method of RNA interference (RNA_i) to reduce caveolin-1 expression. A sequence fragment of human caveolin-1 was chosen and inserted into an EGFP-expressing vector designed for use in RNA_i. Five days following transient transfection of BEC, the

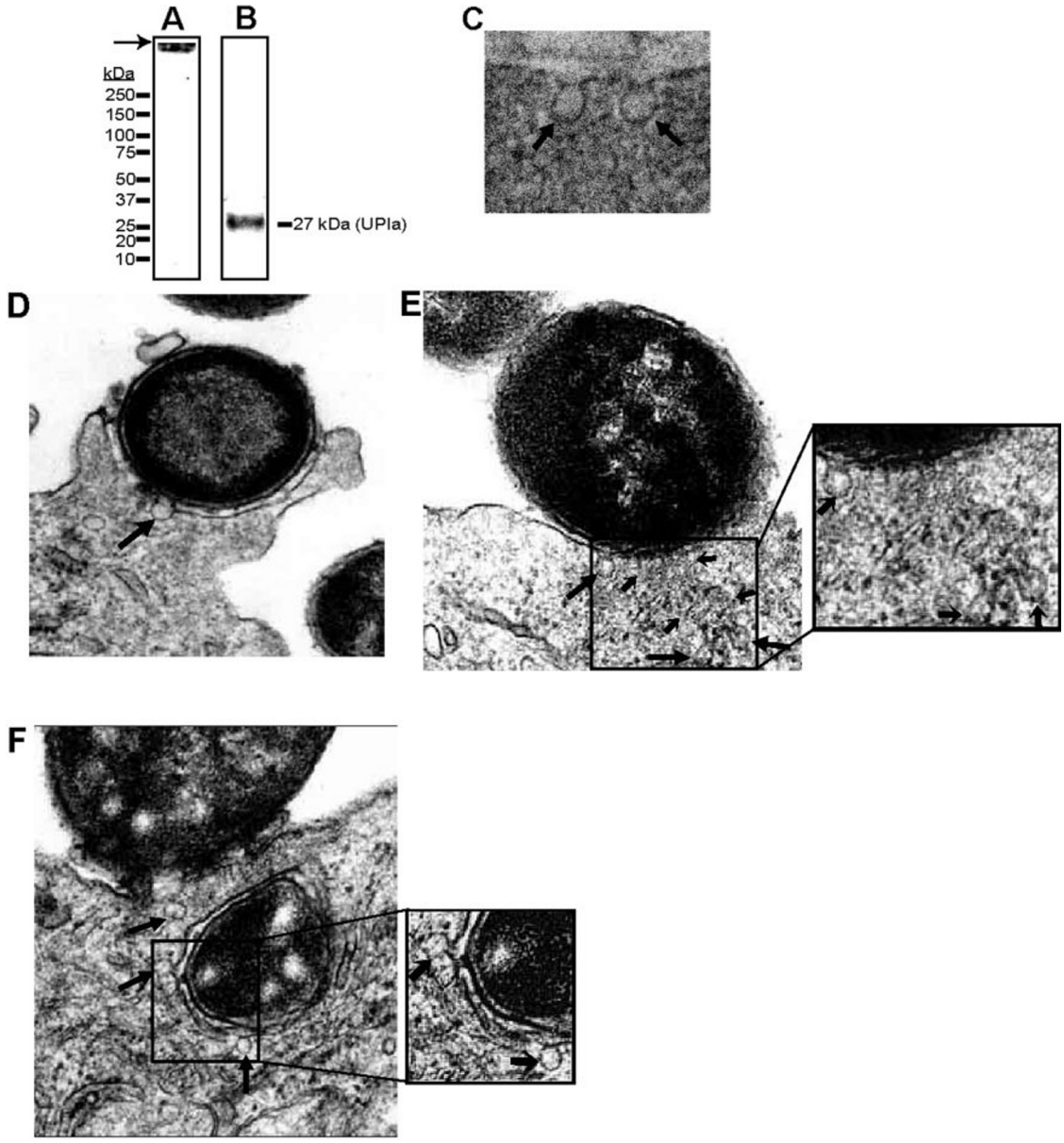

FIG. 1. **5637 human BEC express the *E. coli* type 1 fimbrial receptor, UPIa, and induction of caveolae by type 1 fimbriae-expressing *E. coli*.** *A* and *B*, UPIa-specific Western blot of a 5637 human BEC whole cell lysate in 2× Laemmli sample buffer either boiled (*A*) or incubated at room temperature (*B*) for 30 min. *Arrow* in *A* points to high molecular weight UPIa aggregate. *C*, transmission electron micrograph showing caveolae (*arrows*) on the basolateral surface of 5637 BEC. *D–F*, transmission electron micrographs of 5637 BEC infected with *E. coli* ORN103(pSH2). Note the flask-shaped caveolae associated with bacteria attached to the surface (*arrows* in *D–F*) and with internalized bacteria (*arrows* in *F*; see *inset* of *F*). An interesting structure (*outlined* by *small arrows* in *E*; see *inset* of *E*) associated with a bacterium in the early stages of invasion may represent a "leading edge" of the internalization process.

cells were examined microscopically for the expression of vector-encoded EGFP (*green*) and endogenous caveolin-1 (*red*) using a polyclonal anti-caveolin antibody. Fig. 3, *A* and *B,* show vector (pEGFP-N1A-U6)-transfected cells showing EGFP expression and caveolin-1 labeling (Fig. 3*A*) or caveolin-1 labeling alone (Fig. 3*B*). Note that even cells expressing high levels of EGFP show no changes in caveolin-1 expression. Shown in Fig. 3, *C* and *D,* are RNA_i construct (pSi-Cav419)-transfected cells showing EGFP expression and caveolin-1 labeling (Fig. 3*C*) or caveolin-1 labeling alone (Fig. 3*D*). Note the transfected, EGFP-expressing cells marked with *white arrows* and the large decrease of caveolin-1 expression seen in these cells (Fig. 3, *C–D*). Caveolin-1 expression was quantified by Western blotting and densitometry (Fig. 3*E*). When corrected for protein loading by using the relative amounts of β-actin in each sample, caveolin-1 expression was reduced by ~38%, which corresponded closely with the percentage of cells transfected with pSi-Cav419 (34.3%) (transfection was 28.1% for the vector pEGFP-N1A-U6). When compared with the greater than 50% inhibition of *E. coli* invasion by transfecting with pSi-Cav419, as determined by utilizing a gentamicin protection assay, this indicates an important role for the lipid raft protein caveolin-1 in the process of BEC invasion by *E. coli* (Fig. 3*F*).

Rac1 Associates with Caveolin-1 in Lipid Rafts of BEC—Many signaling molecules are known to be enriched within lipid rafts (20, 23, 24), so we hypothesized that, if lipid rafts are the path of BEC invasion for *E. coli*, signaling molecules involved in *E. coli* invasion of BEC may also be located in lipid rafts. The Rho family GTPase member Rac1 has been shown recently (31) to play a vital role in the invasion of *E. coli* into BEC. We sought to determine whether this signaling molecule, essential to *E. coli* BEC invasion, was also localized to BEC

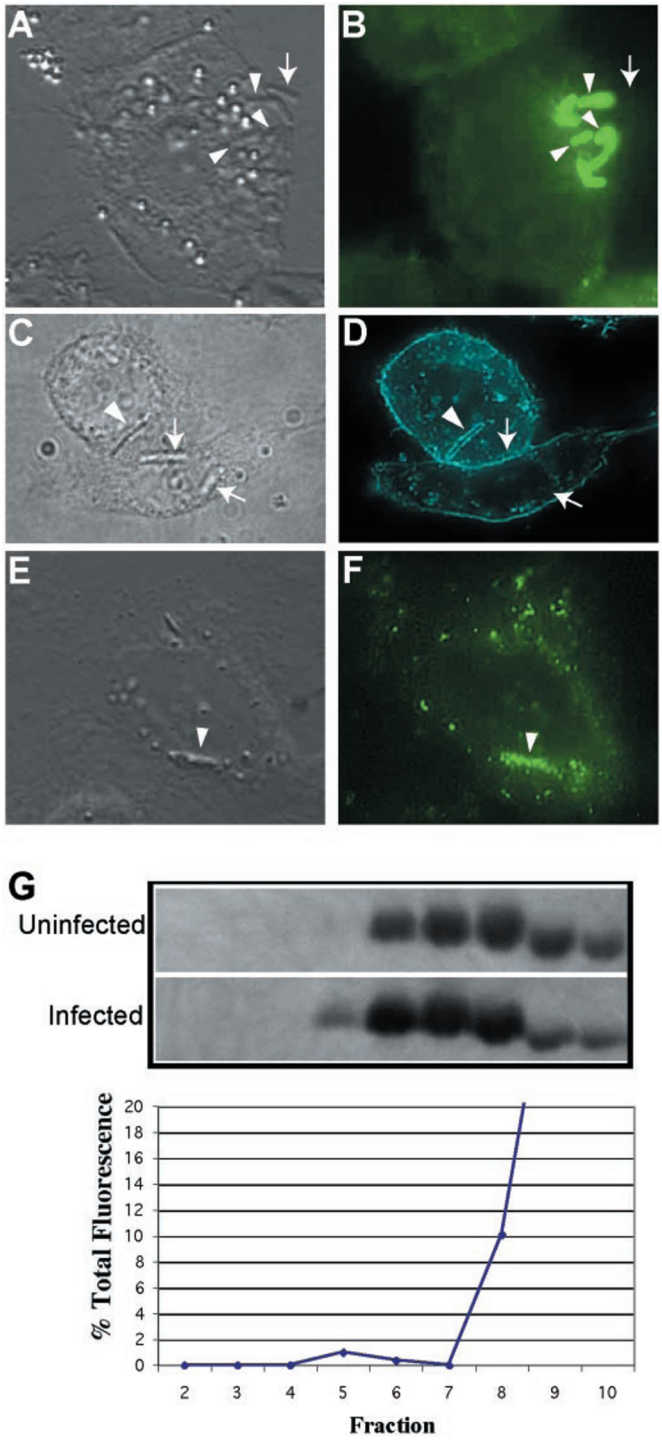

FIG. 2. **Association of internalized type 1 fimbriae-expressing *E. coli* with markers of lipid rafts.** *A–F*, microscopic images showing the association of caveolin-1 (*B*), cholesterol (*D*), and GM1 (*F*) with internalized type 1 fimbriated *E. coli* and the corresponding differential interference contrast images (*A*, *C*, and *E*). *Arrowheads* point to intracellular bacteria, and *arrows* point to extracellular bacteria, which show no labeling. *G*, anti-caveolin-1 Western blot (*top*) and fluorescence content (*bottom*) of fractions from sucrose density gradients of uninfected bladder epithelial cells or cells infected with FITC-labeled *E. coli* ORN103(pSH2).

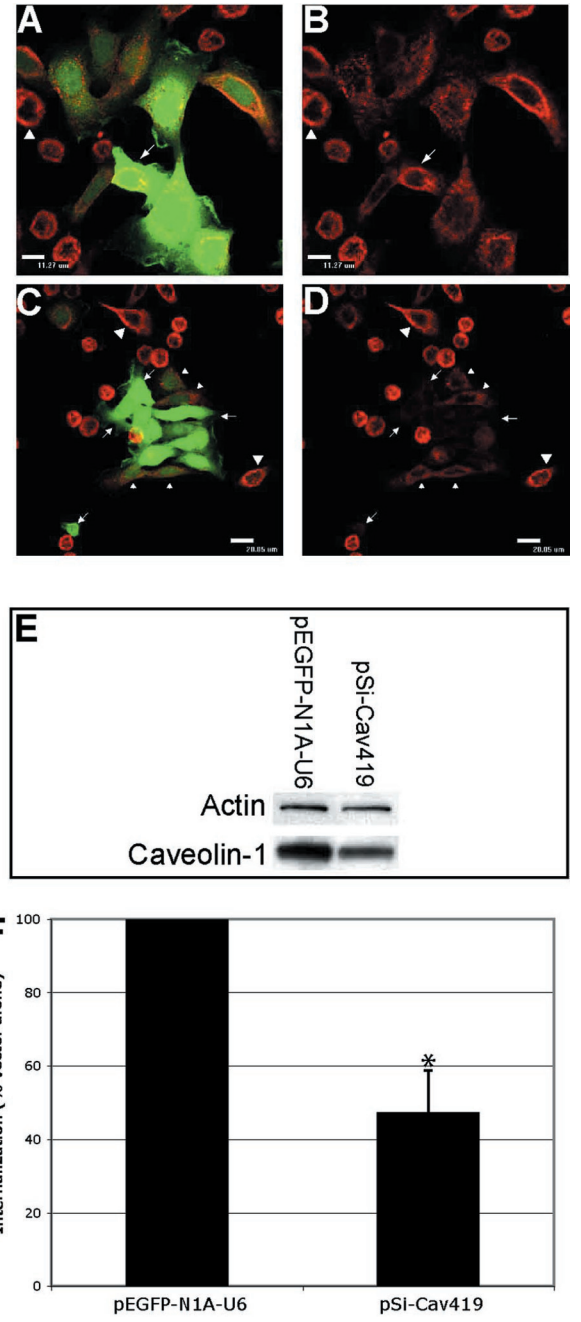

FIG. 3. **RNA$_i$ knockdown of caveolin-1 expression inhibits *E. coli* invasion of BEC.** *A–D*, confocal images of 5637 human BEC transiently transfected with vector alone (pEGFP-N1A-U6) (*A* and *B*) or RNA$_i$ construct (pSi-Cav419) (*C* and *D*). Shown in *A* and *C* is EGFP (*green*) expression and caveolin-1 expression (*red*). Shown in *B* and *D* is caveolin-1 expression (*red*) alone. *White arrows* in *A* and *B* show cells highly transfected with pEGFP-N1A-U6 whose caveolin-1 expression is not altered compared with nontransfected cells (*white arrowhead*). *White arrows* in *C* and *D* show cells highly transfected with pSi-Cav419 whose caveolin-1 expression has been "knocked down." *Small arrowheads* show moderately transfected cells, and *large arrowheads* point to nontransfected cells. *E*, Western blot of 5-day post-transfection 5637 BEC showing relative amounts of β-actin and caveolin-1. *F*, *E. coli* ORN103(pSH2) invasion of 5637 BEC, 5 days after transfection with pEGFP-N1A-U6 or pSi-Cav419. The values are expressed as a percentage of bacterial invasion of pEGFP-N1A-U6 transfected cells. * indicates $p = 0.001$ relative to pEGFP-N1A-U6 transfected cells as determined by Student's *t* test.

lipid rafts. We utilized a lipid raft isolation protocol to purify lipid raft microdomains from uninfected 5637 BEC before and after treatment with the compound MBCD, which extracts cholesterol from the cells, disrupting lipid raft structure and function (35, 36). Following sucrose density gradient centrifugation, the majority of Rac1 (~94% by densitometry) was located in the lipid raft fractions (fractions 4–6), as defined by a light buoyant density and the presence of the lipid raft marker caveolin-1 (~83% by densitometry) (Fig. 4*A*) (29, 39). Following

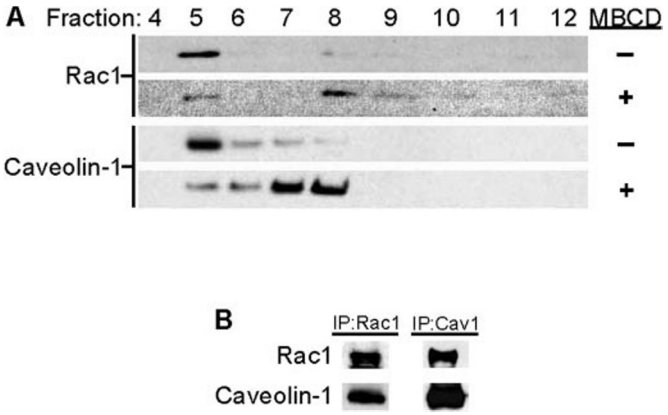

FIG. 4. **The signaling molecule Rac1, required for *E. coli* BEC invasion, is located in BEC lipid rafts.** *A*, Rac1- or caveolin-1-specific Western blot on fractions of uninfected 5637 human BEC isolated by sucrose density fractionation before and after treatment with MBCD. *B*, Rac1- or caveolin-1-specific Western blotting following Rac1- or caveolin-1-specific immunoprecipitation performed on fraction 5 from the sucrose density gradient as shown in *A*.

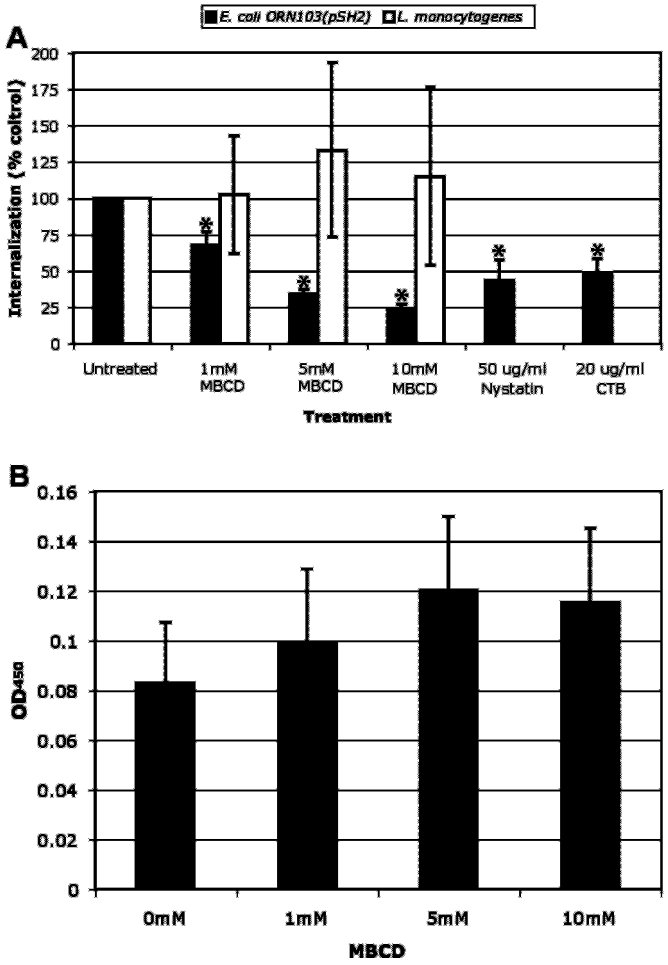

FIG. 5. **Inhibiting invasion into human bladder epithelial cells by disrupting or usurping the function of lipid rafts.** *A*, *E. coli* ORN103(pSH2) or *L. monocytogenes* invasion of bladder epithelial cells before or after 30 min of treatment with MBCD, nystatin, or CTB. The values are expressed as a percentage of bacterial invasion of untreated cells. *B*, the adherence of *E. coli* ORN103(pSH2) to 5637 cells before and after treatment of the cells with MBCD as determined by an MTT-based adherence assay. * indicates $p = 0.001$ relative to untreated controls as determined by Student's *t* test.

treatment with 10 mM MBCD for 1 h, there was a 78% decrease in Rac1 localization and a 70% decrease in caveolin-1 localization to the lipid raft fractions, showing that Rac1 lipid raft localization is sensitive to lipid raft disruption. We further examined the association between Rac1 and caveolin-1 through immunoprecipitation studies of BEC lipid raft fractions. Caveolin-1 was coprecipitated with Rac1-specific immunoprecipitation and vice versa (Fig. 4*B*). We have now demonstrated that a signaling molecule (Rac1) essential for *E. coli* invasion of BEC is located in lipid rafts, implicating these structures as the location where at least a part of the cellular signaling required for *E. coli* BEC invasion is initiated. Together with the data presented in Fig. 3, we have now demonstrated the lipid raft localization of two separate proteins, caveolin-1 and Rac1, that are required for the invasion of BEC by *E. coli*.

Disruptors and Usurpers of Lipid Rafts Block Entry of E. coli into BEC—To demonstrate conclusively the involvement of BEC lipid rafts in *E. coli* invasion, we examined the effect of BEC lipid raft disruption on bacterial invasion. Following a preinfection treatment of BEC with increasing concentrations of MBCD, we observed a dose-dependent inhibition of *E. coli* invasion (Fig. 5*A*), whereas no effect on the entry of *L. monocytogenes* was seen. The invasive bacterium *L. monocytogenes,* which does not normally colonize the bladder, was used solely to demonstrate the specificity of MBCD for inhibiting *E. coli* BEC invasion. Treatment of BEC with MBCD was also not found to cause a decrease in the adherence of *E. coli* to BEC (Fig. 5*B*). *E. coli* invasion was also inhibited by pretreatment with nystatin, another disruptor of lipid rafts (Fig. 5*A*) (36, 40). In addition, pretreatment of BEC with the B subunit of cholera toxin, which enters cells through lipid rafts, thereby making them unavailable to the infecting bacteria, also inhibited *E. coli* invasion (Fig. 5*A*) (35, 41). Thus, specific disruption or occupation of BEC lipid rafts inhibits the entry of *E. coli* into human BEC, conclusively demonstrating that *E. coli* are utilizing lipid rafts as the portal of entry into BEC *in vitro*. We next sought to confirm our results by demonstrating *E. coli* invasion of BEC via lipid rafts *in vivo*, using a well established mouse model of UTI (9, 10, 42).

Association of Uroplakin Ia with Lipid Rafts in the Mouse Bladder—It has been hypothesized previously (25, 43) that for microbial invasion via lipid rafts to occur, the host cell receptor must either be located in lipid rafts or move to lipid rafts after microbial attachment. We therefore sought to determine whether the receptor for type 1 fimbriated *E. coli* on mouse BEC, UPIa, was associated with lipid rafts by purifying lipid raft microdomains from the bladders of BALB/c mice. The majority of UPIa (~81% by densitometry) is found in the light buoyant density fractions (fractions 4–6) along with the lipid raft protein caveolin-1 (~59% by densitometry), well separated from the heavy chain of clathrin, a non-lipid raft protein associated with clathrin-coated pits, that is located in fractions 11 and 12 (Fig. 6*A*) (35). Thus, the BEC receptor for *E. coli* type 1 fimbriae has been isolated in the lipid raft fractions of the mouse bladder, leading us to further study the role of lipid rafts in mediating *E. coli* invasion of mouse BEC *in vivo*.

Inhibition of E. coli BEC Invasion in Vivo—We examined the effect of lipid raft disruption on *E. coli* invasion of mouse BEC by using the agent MBCD in a mouse UTI model (42). Uropathogenic type 1 fimbriated *E. coli* J96 (28) suspended in 25 mM MBCD in PBS, or in PBS alone, was instilled into the bladders of mice. After 1 h, the bladders were removed, bisected, and incubated for 1 h in the presence of the antibiotic gentamicin to kill extracellular bacteria. MBCD had no effect on bacterial viability as determined by colony counts after a 60-min incubation in PBS with or without 25 mM MBCD. MBCD treatment was found to inhibit markedly the invasion of BEC by *E. coli* J96, but had no effect on the invasion of BEC by the bacteria *L. monocytogenes*, which was again used as a

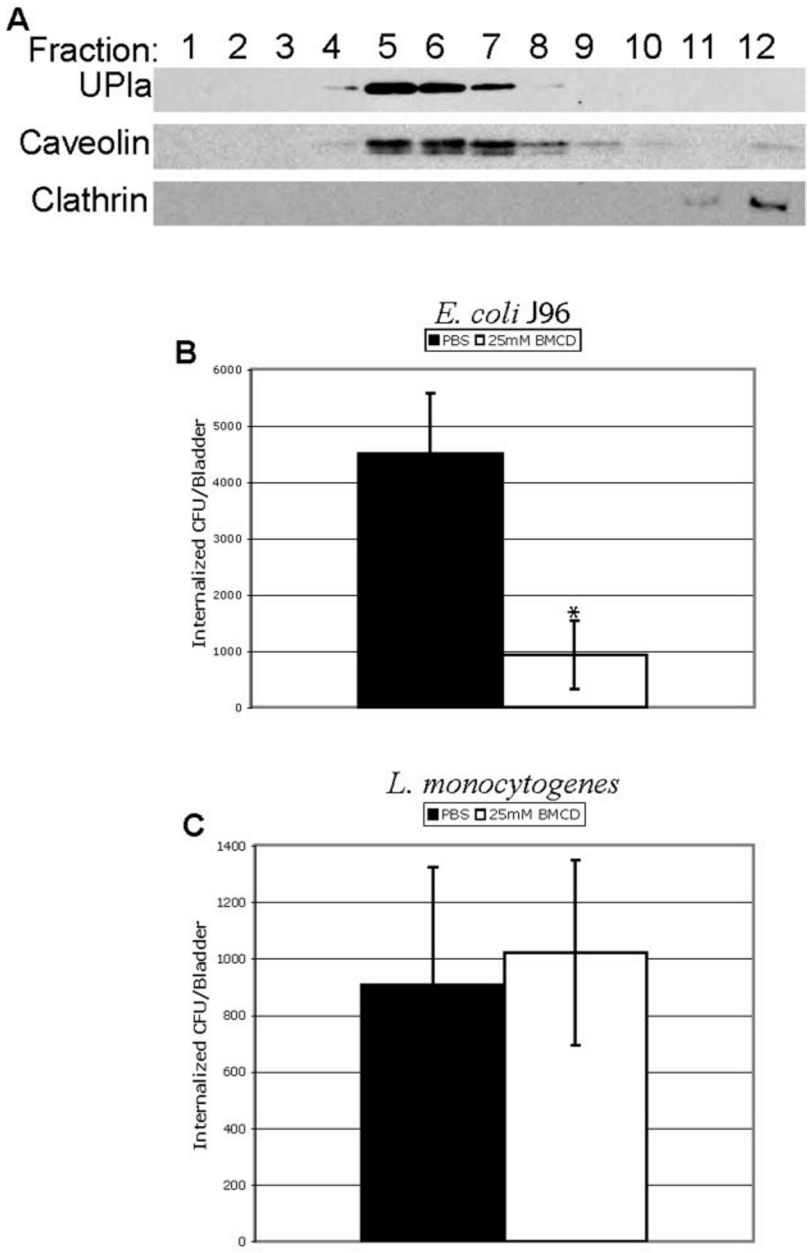

FIG. 6. ***E. coli* invades mouse BEC via lipid rafts in a mouse model of UTI.** *A*, UPIa, caveolin-1, or clathrin heavy chain-specific Western blotting of mouse bladder fractions purified by sucrose density fractionation. *B* and *C*, invasion of BEC in a mouse model of UTI by *E. coli* J96 (*B*) or *L. monocytogenes* (*C*) in the presence or absence of 25 mM MBCD. * indicates $p = 0.001$ relative to mice infected in the absence of MBCD as determined by Student's *t* test. *B* and *C*, $n = 5$ mice per group.

control for the specificity of MBCD inhibition of *E. coli* BEC invasion (Fig. 6, *B* and *C*). Thus, by disrupting mouse BEC lipid rafts, we were able to specifically block the invasion of BEC by *E. coli*, demonstrating that lipid rafts mediate *E. coli* BEC invasion *in vivo* and implying a therapeutic potential for the management of UTIs.

DISCUSSION

Uropathogens are thought to persist in a reservoir located in the gastrointestinal tract and to initiate infection by being introduced into the urethra (8). It is becoming apparent that the bladder itself can serve as a reservoir, with the bacteria invading the uroepithelium and persisting intracellularly in a quiescent state, later reemerging to initiate another round of infection (9–11). The findings presented here demonstrate by morphological, biochemical, and functional analysis that *E. coli* invasion of BEC utilizes host cell lipid rafts.

The involvement of lipid rafts in bacterial invasion of 5637 human BEC *in vitro* was first indicated by the intimate association seen between invading bacteria and host cell caveolae. The expression of caveolae is normally restricted to the basolateral surface of uninfected BEC, but invading *E. coli* were seen to induce the formation of caveolar structures at sites of bacterial attachment. The association of *E. coli* with caveolar structures is somewhat reminiscent of the early stages of host cell infection by simian virus 40 and echovirus 1, where viral particles have been shown to interact with host cell caveolae by TEM (38, 40). The association of lipid rafts with intracellular bacteria was further demonstrated by fluorescent microscopy, using specific probes for three commonly used markers of lipid rafts, and by biochemical means, showing association between bacteria-containing phagosomes and the lipid raft protein caveolin-1. The association of lipid rafts markers with intracellular *E. coli* in BEC is consistent with previous work demonstrating microbial infection/invasion of host cells via lipid rafts (25, 35, 36), and led us to examine the role of a known lipid raft protein, caveolin-1, in *E. coli* invasion. Caveolin-1, which is required for the formation of caveolar structures (30, 44), was found to be required for the invasion of *E. coli* into BEC, because inhibiting the expression of caveolin-1 by RNA_i also inhibited invasion of BEC by *E. coli*. The exact mechanism

through which caveolin-1 functions in this event is not known, but this protein has been shown to interact with a number of different signaling molecules and is tyrosine-phosphorylated during certain signaling events (23, 24, 45). The Rho family GTPase member Rac1, a signaling molecule involved in actin polymerization and shown previously to be required for *E. coli* BEC invasion, was also shown to be located in BEC lipid rafts and was associated with caveolin-1 by immunoprecipitation. Determining what effect this caveolin-1/Rac1 interaction has on *E. coli* BEC invasion will require further study, but it has been demonstrated that lipid raft localization is required for proper stretch-induced Rac1 activation in cardiomyocytes (39).

The *E. coli* type 1 fimbrial receptor on BEC is the protein UPIa (15), one of the four uroplakins that make up the scallop-shaped urothelial plaques, which are thought to play an important role in determining the permeability barrier presented by the uroepithelium (14). In this report, we have demonstrated for the first time an association between UPIa and biochemically purified lipid rafts isolated from mouse bladders, as well as the MBCD inhibition of BEC invasion by *E. coli* in a mouse model of UTI. The ability of type 1 fimbriated *E. coli* to invade BEC appears to play a large role in the pathogenesis of UTIs as well as the recurrence of these infections (9–11, 42). Understanding the role host cell lipid rafts play in the invasion of type 1 fimbriated *E. coli* into BEC would allow for a better understanding of how to break the cycle of infection and recurrence so common to UTIs. A clinical correlation has been made between elevated serum cholesterol and an increased incidence of UTI (46), which, along with our results, suggests that the use of agents that modulate cellular cholesterol could play a role in the management of UTIs. Indeed, many such agents, including methyl-β-cyclodextrin, have already been safely used in humans (47).

It is important to note that the high impermeability of the bladder epithelium is thought to be mediated not only by the urothelial plaques but also by the specialized composition of the lipids associated with them (14, 18–22). Thus, the urothelial plaques and their associated lipid microdomains seem to serve complementary roles in mediating the impressive impermeability of the bladder epithelium. We hypothesize that, paradoxically, *E. coli* is utilizing two mediators of uroepithelial impermeability, namely the uroplakin particle (specifically UPIa) and their associated cholesterol/sphingolipid enriched microdomains to penetrate the bladder epithelium. The uroplakin particles themselves undergo physiological endocytosis and exocytosis initiated by uroepithelial stretching and relaxation that occurs during normal filling and emptying of the bladder (48, 49), and lipid rafts are known to contain the molecular machinery required for endocytosis (50). It is not known whether lipid rafts and associated molecules play some role in the normal endocytosis/exocytosis of uroplakin particles, but it now seems possible that *E. coli* could be usurping this particular feature of uroplakin particles in a nonphysiological manner to bypass the uroepithelial barrier.

Acknowledgments—We thank Brian Bishop and James McLachlan for critical review of the manuscript and Todd Gambling for assistance with transmission EM.

REFERENCES

1. Barnett, B. J., and Stephens, D. S. (1997) *Am. J. Med. Sci.* **314,** 245–249
2. Hooton, T. M., and Stamm, W. E. (1997) *Infect. Dis. Clin. North Am.* **11,** 551–581
3. Svanborg, C., and Godaly, G. (1997) *Infect. Dis. Clin. North Am.* **11,** 513–529
4. Abraham, S. N., Sun, D., Dale, J. B., and Beachey, E. H. (1988) *Nature* **336,** 682–684
5. Connell, I., Agace, W., Klemm, P., Schembri, M., Marild, S., and Svanborg, C. (1996) *Proc. Natl. Acad. Sci. U. S. A.* **93,** 9827–9832
6. Stapleton, A. (1999) *Adv. Exp. Med. Biol.* **462,** 351–358
7. Foxman, B. (1990) *Am. J. Public Health* **80,** 331–333
8. Hooton, T. M. (2001) *Int. J. Antimicrob. Agents* **17,** 259–268
9. Mulvey, M. A., Schilling, J. D., and Hultgren, S. J. (2001) *Infect. Immun.* **69,** 4572–4579
10. Schilling, J. D., Lorenz, R. G., and Hultgren, S. J. (2002) *Infect. Immun.* **70,** 7042–7049
11. Martinez, J. J., Mulvey, M. A., Schilling, J. D., Pinkner, J. S., and Hultgren, S. J. (2000) *EMBO J.* **19,** 2803–2812
12. Lewis, S. A., and Diamond, J. M. (1976) *J. Membr. Biol.* **28,** 1–40
13. Lewis, S. A. (2000) *Am. J. Physiol.* **278,** F867–F874
14. Hu, P., Meyers, S., Liang, F. X., Deng, F. M., Kachar, B., Zeidel, M. L., and Sun, T. T. (2002) *Am. J. Physiol.* **283,** F1200–F1207
15. Zhou, G., Mo, W. J., Sebbel, P., Min, G., Neubert, T. A., Glockshuber, R., Wu, X. R., Sun, T. T., and Kong, X. P. (2001) *J. Cell Sci.* **114,** 4095–4103
16. Wu, X. R., Medina, J. J., and Sun, T. T. (1995) *J. Biol. Chem.* **270,** 29752–29759
17. Krylov, A. V., Pohl, P., Zeidel, M. L., and Hill, W. G. (2001) *J. Gen. Physiol.* **118,** 333–340
18. Vergara, J., Zambrano, F., Robertson, J. D., and Elrod, H. (1974) *J. Cell Biol.* **61,** 83–94
19. Ketterer, B., Hicks, R. M., Christodoulides, L., and Beale, D. (1973) *Biochim. Biophys. Acta* **311,** 180–190
20. Brown, D. A., and London, E. (2000) *J. Biol. Chem.* **275,** 17221–17224
21. Lande, M. B., Donovan, J. M., and Zeidel, M. L. (1995) *J. Gen. Physiol.* **106,** 67–84
22. Simons, K., and Ikonen, E. (1997) *Nature* **387,** 569–572
23. Anderson, R. G. (1998) *Annu. Rev. Biochem.* **67,** 199–225
24. Couet, J., Belanger, M. M., Roussel, E., and Drolet, M. C. (2001) *Adv. Drug Delivery Rev.* **49,** 223–235
25. Duncan, M. J., Shin, J. S., and Abraham, S. N. (2002) *Cell Microbiol.* **4,** 783–791
26. van der Goot, F. G., and Harder, T. (2001) *Semin. Immunol.* **13,** 89–97
27. Orndorff, P. E., and Falkow, S. (1984) *J. Bacteriol.* **159,** 736–744
28. Svanborg Eden, C., Hull, R., Falkow, S., and Leffler, H. (1983) *Prog. Food Nutr. Sci.* **7,** 75–89
29. Song, K. S., Li, S., Okamoto, T., Quilliam, L. A., Sargiacomo, M., and Lisanti, M. P. (1996) *J. Biol. Chem.* **271,** 9690–9697
30. Vogel, U., Sandvig, K., and van Deurs, B. (1998) *J. Cell Sci.* **111,** 825–832
31. Martinez, J. J., and Hultgren, S. J. (2002) *Cell Microbiol.* **4,** 19–28
32. Schilling, J. D., Mulvey, M. A., Vincent, C. D., Lorenz, R. G., and Hultgren, S. J. (2001) *J. Immunol.* **166,** 1148–1155
33. Schilling, J. D., Martin, S. M., Hunstad, D. A., Patel, K. P., Mulvey, M. A., Justice, S. S., Lorenz, R. G., and Hultgren, S. J. (2003) *Infect. Immun.* **71,** 1470–1480
34. Wu, X. R., Manabe, M., Yu, J., and Sun, T. T. (1990) *J. Biol. Chem.* **265,** 19170–19179
35. Shin, J. S., Gao, Z., and Abraham, S. N. (2000) *Science* **289,** 785–788
36. Baorto, D. M., Gao, Z., Malaviya, R., Dustin, M. L., van der Merwe, A., Lublin, D. M., and Abraham, S. N. (1997) *Nature* **389,** 636–639
37. Roy, S., Luetterforst, R., Harding, A., Apolloni, A., Etheridge, M., Stang, E., Rolls, B., Hancock, J. F., and Parton, R. G. (1999) *Nat. Cell Biol.* **1,** 98–105
38. Marjomaki, V., Pietiainen, V., Matilainen, H., Upla, P., Ivaska, J., Nissinen, L., Reunanen, H., Huttunen, P., Hyypia, T., and Heino, J. (2002) *J. Virol.* **76,** 1856–1865
39. Kawamura, S., Miyamoto, S., and Brown, J. H. (2003) *J. Biol. Chem.* **278,** 31111–31117
40. Anderson, H. A., Chen, Y., and Norkin, L. C. (1996) *Mol. Biol. Cell* **7,** 1825–1834
41. Naroeni, A., and Porte, F. (2002) *Infect. Immun.* **70,** 1640–1644
42. Mulvey, M. A., Lopez-Boado, Y. S., Wilson, C. L., Roth, R., Parks, W. C., Heuser, J., and Hultgren, S. J. (1998) *Science* **282,** 1494–1497
43. Shin, J. S., and Abraham, S. N. (2001) *Science* **293,** 1447–1448
44. Razani, B., Engelman, J. A., Wang, X. B., Schubert, W., Zhang, X. L., Marks, C. B., Macaluso, F., Russell, R. G., Li, M., Pestell, R. G., Di Vizio, D., Hou, H., Jr., Kneitz, B., Lagaud, G., Christ, G. J., Edelmann, W., and Lisanti, M. P. (2001) *J. Biol. Chem.* **276,** 38121–38138
45. Mastick, C. C., Brady, M. J., and Saltiel, A. R. (1995) *J. Cell Biol.* **129,** 1523–1531
46. Gulati, S., Kher, V., Arora, P., Gupta, S., and Kale, S. (1996) *Pediatr. Infect. Dis. J.* **15,** 237–240
47. Toyoda, K., Shoda, T., Uneyama, C., Takada, K., and Takahashi, M. (1997) *Food Chem. Toxicol.* **35,** 331–336
48. Truschel, S. T., Wang, E., Ruiz, W. G., Leung, S. M., Rojas, R., Lavelle, J., Zeidel, M., Stoffer, D., and Apodaca, G. (2002) *Mol. Biol. Cell* **13,** 830–846
49. Lewis, S. A., and de Moura, J. L. (1982) *Nature* **297,** 685–688
50. Schnitzer, J. E., Liu, J., and Oh, P. (1995) *J. Biol. Chem.* **270,** 14399–14404